682 **SUPPLEMENTAL FIGURES**

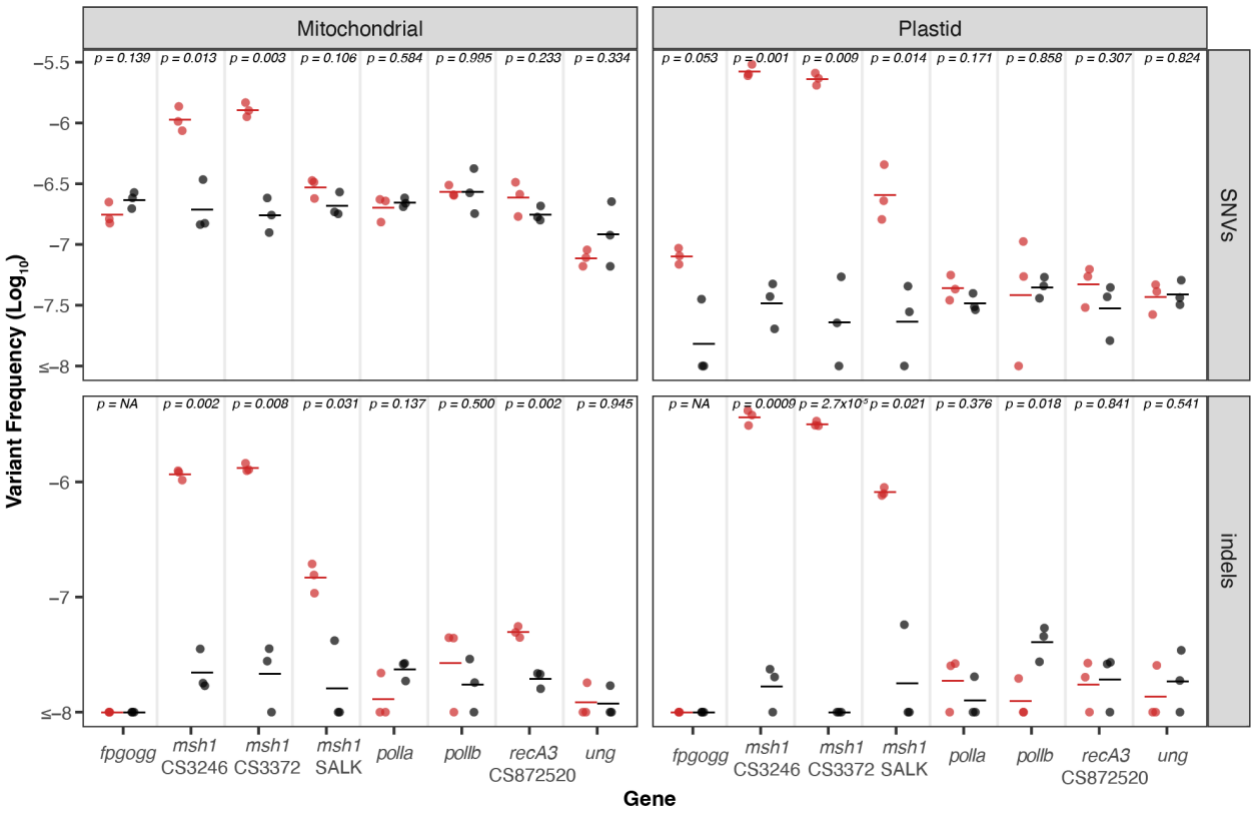

683 Figure S1. *De novo* point mutations measured with Duplex Sequencing from data generated
684 in Wu *et al.* 2020. For each gene of interest (x-axis) mutant lines are plotted in red and
685 matched WT controls are plotted in black. The individual biological replicates are plotted
686 as circles, and group averages are plotted as dashes. Panels separate the data by genome
687 (left column: Mitochondria and right column: Plastid) and by point mutation type (top row:
688 SNVs and bottom row: indels). The y-axis shows the log-transformed SNV frequencies
689 (total SNVs/total DCS coverage). P-values show the result of a two-tailed *t*-test comparing
690 WT vs mutant mutation frequencies for each gene of interest. We found significant
691 increases in SNV and indel frequencies in the *msh1* CS3246 and *msh1* CS3372 mutants
692 (both genomes) but the *msh1* SALK046763 mutant, which is not a complete knockout of
693 the *msh1* gene (Wu *et al.,* 2020) had weaker effects. In addition, we note that this *recA3*
694 null allele is different from the *recA3* null allele that was reported in the new dataset, but
695 both yielded similar results: significant indel and weakly significant SNV increases in
696 mtDNA of the *recA3* mutant. Also note the marginally significant difference in *fpg/ogg*

697 plastid SNVs is explained by just 5 SNVs in mutants and a single SNV in the WT controls,

698 which we do not consider to be a biologically meaningful difference.

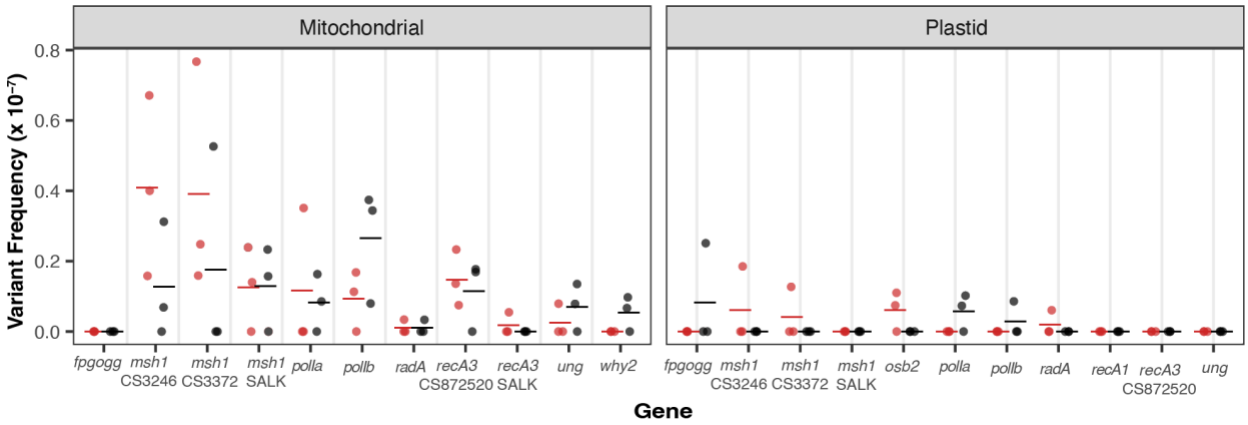

699 Figure S2. Dinucleotide mutations measured with Duplex Sequencing. For each gene of
700 interest (x axis) mutant lines are plotted in red, and matched WT controls are plotted in
701 black. The individual biological replicates are plotted as circles, and group averages are
702 plotted as dashes. Panels divide the data by mitochondrial and plastid. We performed
703 Wilcoxon rank sum tests to look for differences between mutant and matched WT controls
704 and all p-values were > 0.05. Note that *recA3* CS872520 dataset was generated in Wu *et al.*
705 (2020), and the *recA3* SALK 146388 dataset was generated in this study.

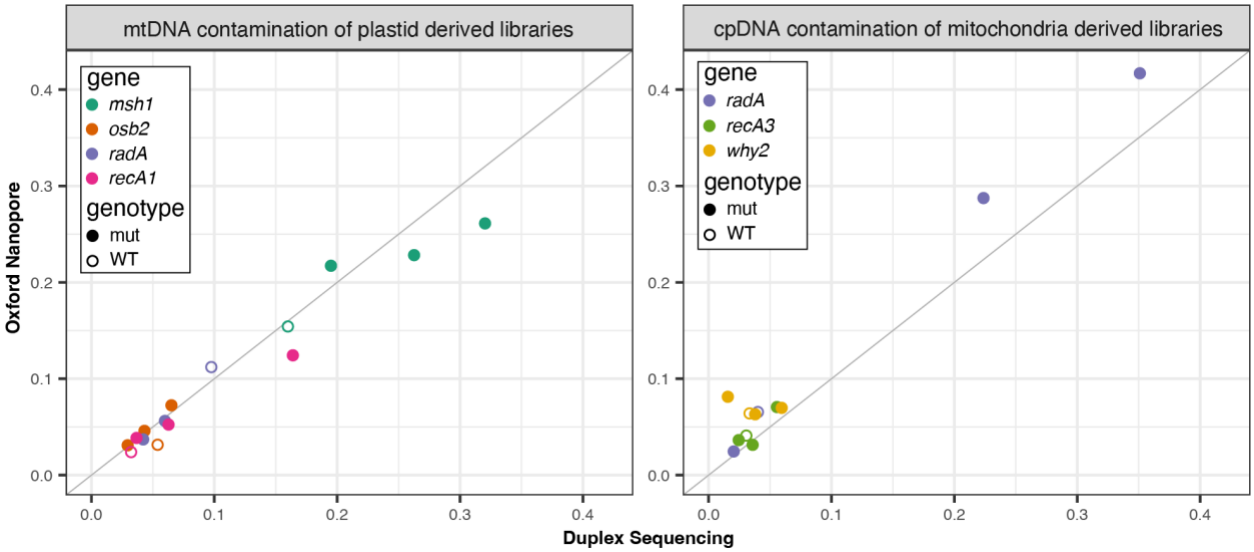

706 Figure S3. Correlation of cross-organelle contamination in Oxford Nanopore and Duplex
707 Sequencing libraries. Contamination is calculated as the number of contaminating reads in
708 the read alignments divided by the total number of organellar alignments. The different
709 mutant lines are colored according to the figure legend with mutant replicates plotted
710 using closed circles and matched WT controls plotted with open circles. The 1:1 diagonal
711 line is shown in gray. Though the level of contamination varies between different DNA
712 samples (for example mtDNA contamination is higher in the plastid derived *msh1* libraries)
713 the contamination levels are generally similar irrespective of sequencing technique. Note,
714 For the *msh1* mtDNA analysis, we relied exclusively the plastid-derived *msh1* samples,
715 and for the *radA* mtDNA analysis, we used a combination of the low coverage *radA*
716 mitochondrial samples and the plastid *radA* samples (see main text).

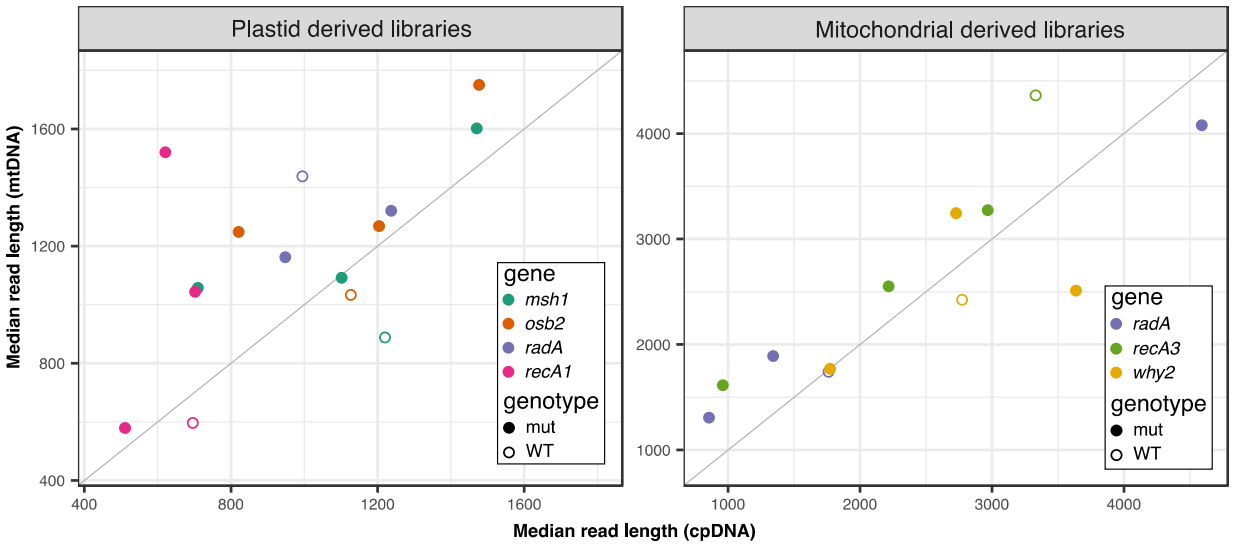

717 Figure S4. Median read length cross-organelle contaminating and native reads in the
718 plastid and mitochondrial derived nanopore libraries. The different mutant lines are
719 colored according to the figure legend with mutant replicates plotted using closed circles
720 and matched WT controls plotted with open circles. The 1:1 diagonal line is show in gray.
721 Note, For the *msh1* mtDNA analysis, we relied exclusively the plastid-derived *msh1*
722 samples, and for the *radA* mtDNA analysis, we used a combination of the low coverage
723 *radA* mitochondrial samples and the plastid *radA* samples (see main text).

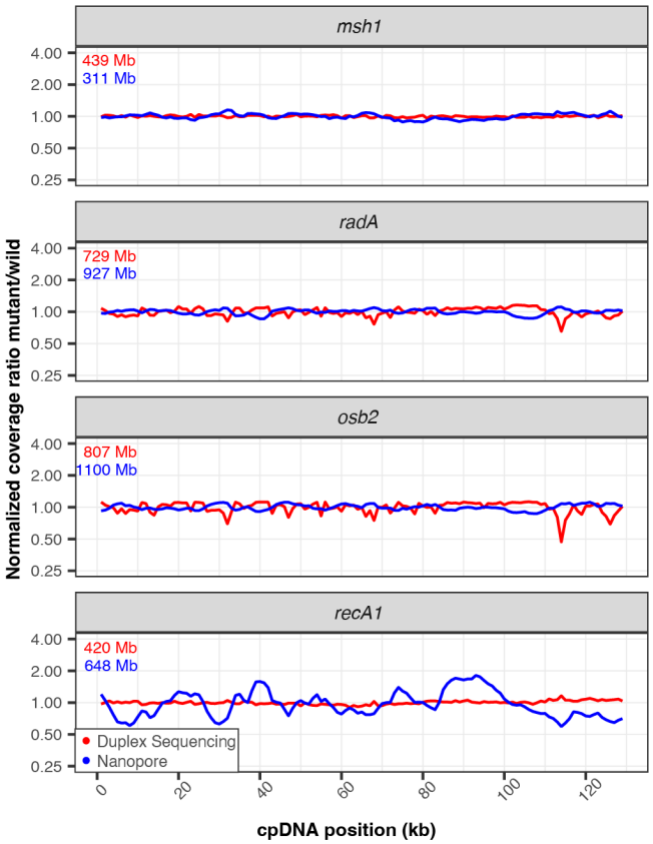

724 Figure S5. Normalized coverage of plastid genomes in mutant lines of interest . Coverage of
725 each Duplex Sequencing (red) or nanopore (blue) library was calculated in 1000-bp
726 windows. Mutant coverage was pooled and divided by WT coverage and the resulting ratios
727 were normalized to 1 for plotting. The total amount of sequencing data used to generate
728 each plot is shown in the top left corner of each panel (red=Duplex Sequencing and
729 blue=nanopore) and is included to highlight the instances where disagreement between
730 the Duplex Sequencing and nanopore lines may be explained by increased variance in the
731 nanopore sample due to lower mtDNA coverage. To see the coverage of the individual
732 replicates see Fig S8 and S9.

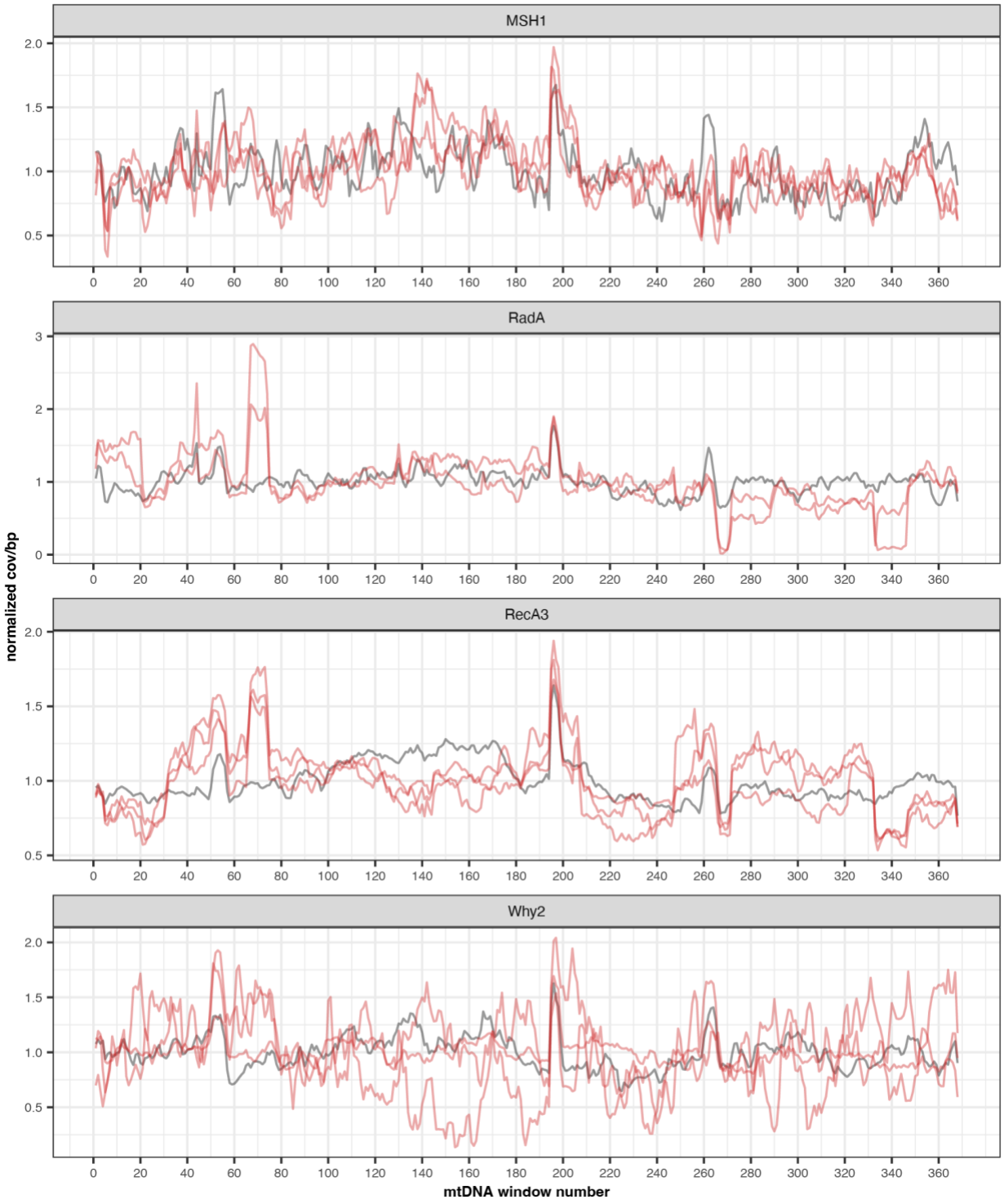

733 Figure S6. Normalized coverage of the individual nanopore mtDNA replicates (used to
734 generate Fig. 8). The red and black lines show the normalized coverage of the mutant
735 replicates and the matched WT control, respectively. Note that variation in the *why2*

736 mutants is likely due to extremely low coverage in these samples (average coverage per bp
737 of 157.3, 6.5 and 7.0 in mutant replicates 1, 2 and 3, respectively).

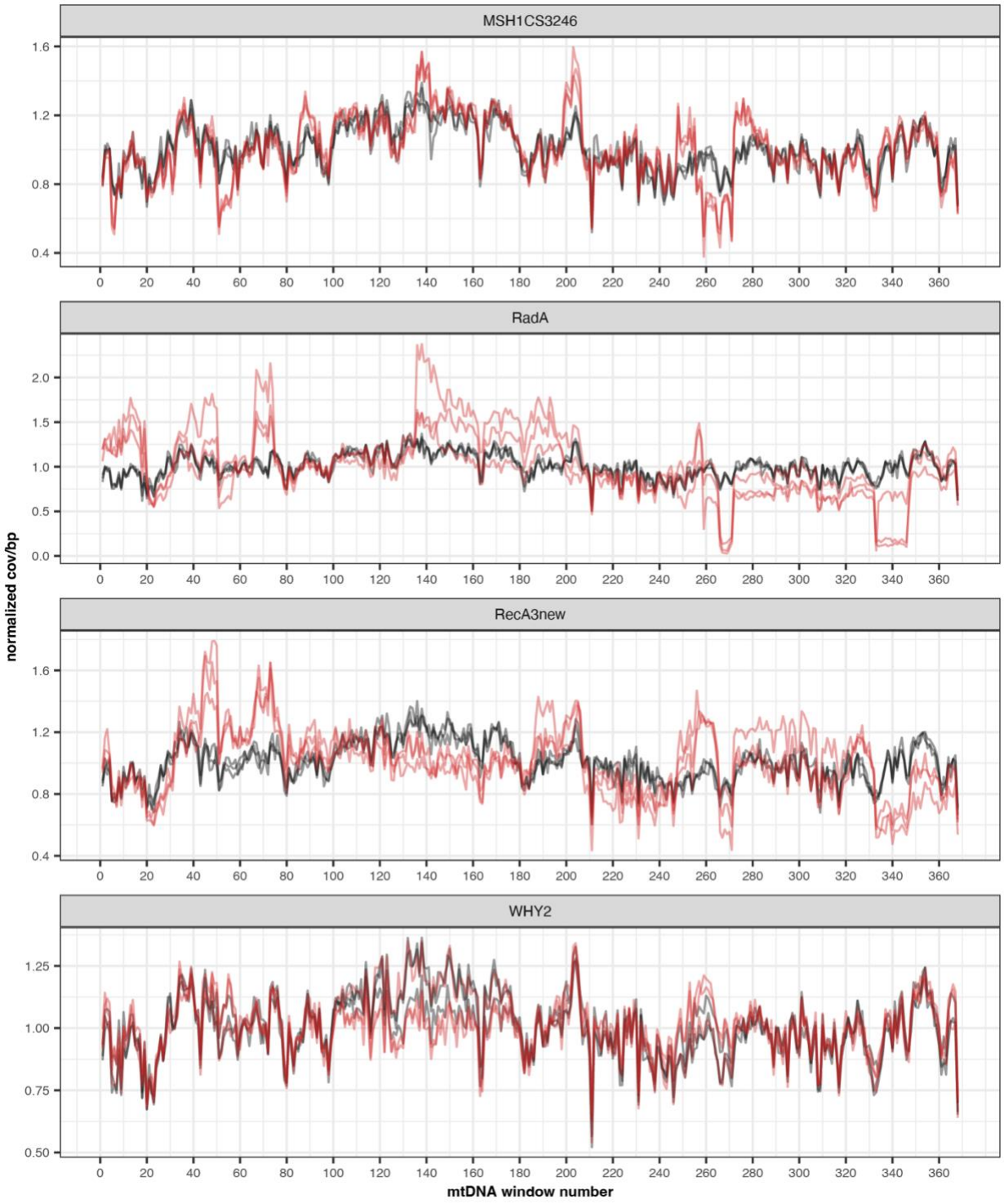

738 Figure S7. Depth of coverage of the individual Duplex Sequencing mtDNA replicates (used
739 to generate Fig. 8). The red and black lines show the normalized coverage of the mutant
740 replicates and the matched WT control, respectively.

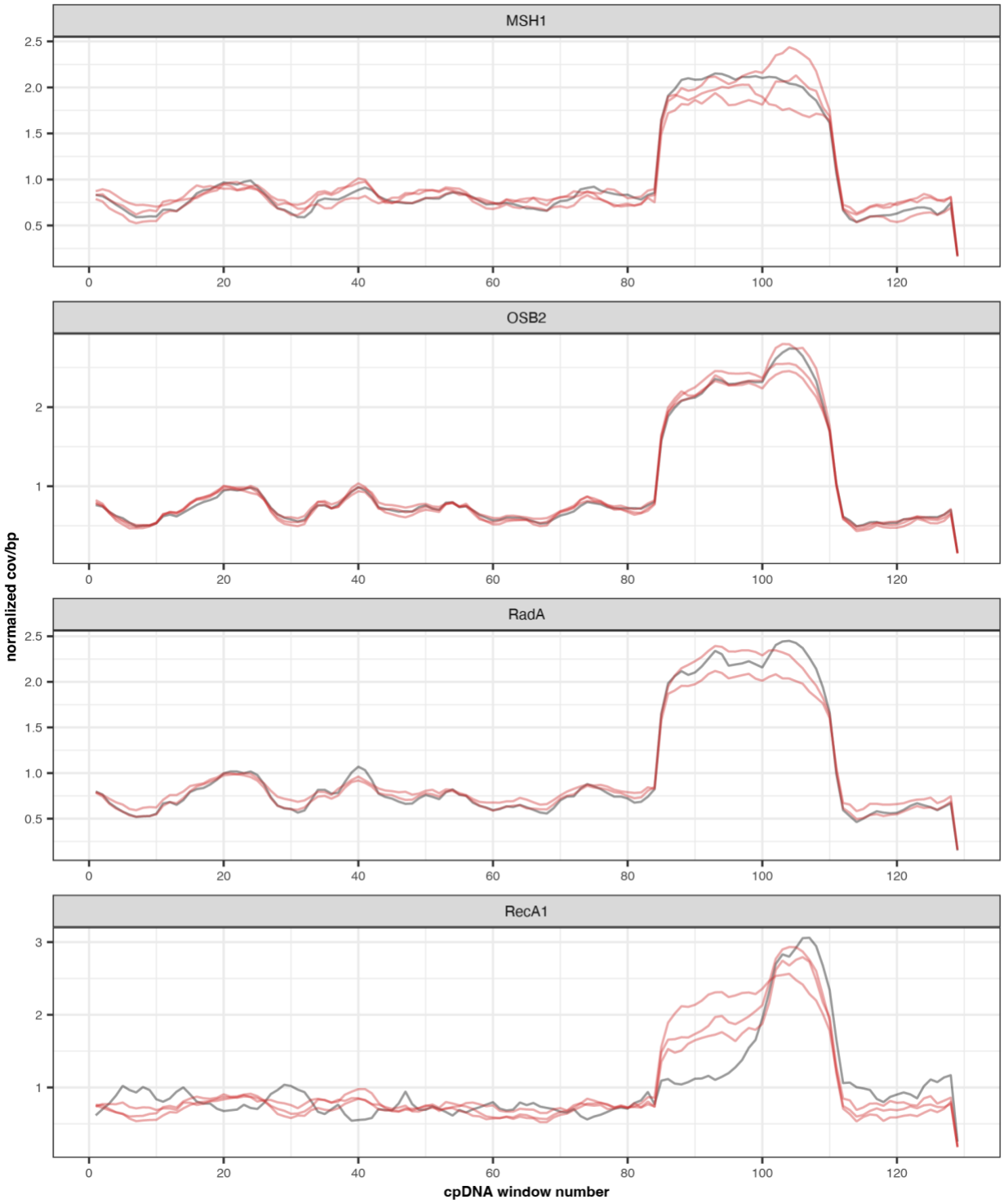

741 Figure S8. Normalized of coverage of the individual nanopore cpDNA replicates (used to
742 generate Fig. 8). The red and black lines show the normalized coverage of the mutant
743 replicates and the matched WT control, respectively. Note that the spike in coverage at
744 ~84-112 kb results from the large inverted repeat, since these reads were mapped

745 noncompetitively with minimap2 (see methods). The second copy of the inverted repeat

746 was omitted for plotting.

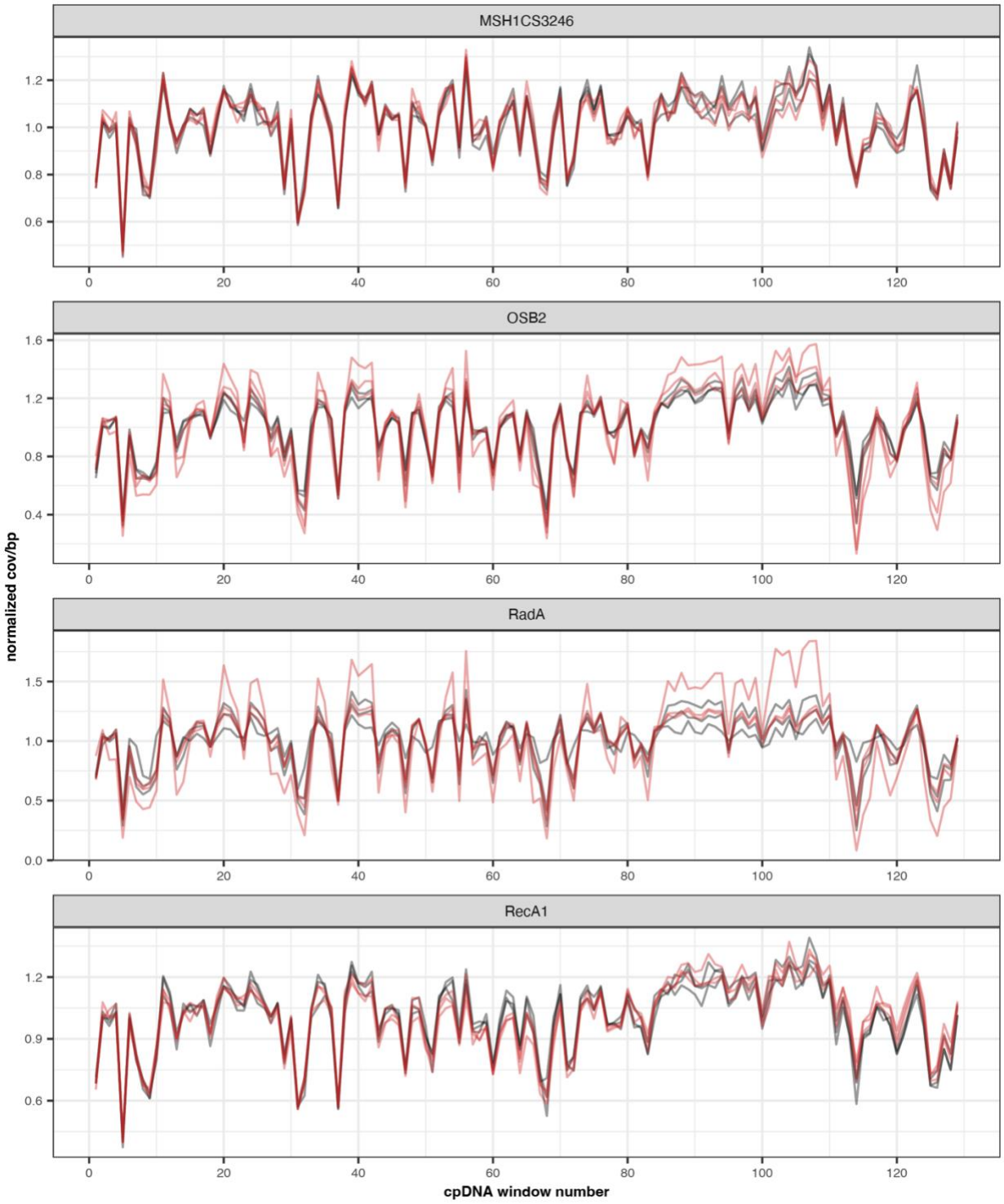

747 Figure S9. Normalized coverage of the individual Duplex Sequencing cpDNA replicates
748 (used to generate Fig. 8). The red and black lines show the normalized coverage of the
749 mutant replicates and the matched WT control, respectively. Note these reads were

750 mapped to a full length cpDNA but the second large inverted repeat was omitted for
751 plotting.

SUPPLEMENTAL TABLES

Table S1. Mutant lines used in this study and primers to verify plant genotype

Gene	Salk line (all from ABRC)	Locus	Forward Primer Wild	Forward Primer Mutant (LBb1.3)	Reverse Primer Wild and Mutant
radA	SALK_097880	AT5G50340	TTTCACTTATCGAGCCAGAGC	ATTTTGCCGATTTCGGAAC	ATGCCATAATGCTTTTTGCTG
recA1	SALK_072979	AT1G79050	TAGGGTGAGATTGGAATGCAG	ATTTTGCCGATTTCGGAAC	AAGAGCTGCTGCTCATCAAAG
recA3	SALK_146388	AT3G10140	CGTTTGGTCAGTTGAAGCTTC	ATTTTGCCGATTTCGGAAC	CTCCACAAGTCACTTCTTCGG
osb2	SALK_061852	AT4G20010	AGCGTGAAAGGTGAGACGTT	ATTTTGCCGATTTCGGAAC	GGGAAATAACAGTACCAGCCC
why2	SALK_118900	AT1G71260	CAGGAAGTCACTGTCAGTTAAGC	ATTTTGCCGATTTCGGAAC	ACCCATGATTTAGAAGTCTTAGAGAGG

755 **Table S2.** Duplex read-pairs and organellar genome coverage

Sample	Count of read-pairs (2x150)	Organellar coverage per bp
mitochondrial_rada_mut_1	75863350	297.9
mitochondrial_rada_mut_2	64771627	281.8
mitochondrial_rada_mut_3	139195192	803.4
mitochondrial_rada_wild_1	70847671	127.8
mitochondrial_rada_wild_2	61998713	246.9
mitochondrial_rada_wild_3	127161861	816.4
mitochondrial_reca3_mut_1	43472074	94.2
mitochondrial_reca3_mut_2	44312097	229.3
mitochondrial_reca3_mut_3	59128403	497.3
mitochondrial_reca3_wild_1	62354817	238.2
mitochondrial_reca3_wild_2	54311915	183.2
mitochondrial_reca3_wild_3	40734051	144.8
mitochondrial_why2_mut_1	63375069	338.0
mitochondrial_why2_mut_2	76906783	284.9
mitochondrial_why2_mut_3	76221972	292.6
mitochondrial_why2_wild_1	68231709	279.8
mitochondrial_why2_wild_2	81396138	379.9
mitochondrial_why2_wild_3	86880259	408.4
plastid_osb2_mut_1	47505179	1176.6
plastid_osb2_mut_2	54307516	870.8
plastid_osb2_mut_3	59415250	898.6
plastid_osb2_wild_1	59542949	1132.8
plastid_osb2_wild_2	69408084	889.7
plastid_osb2_wild_3	67727784	668.6
plastid_rada_mut_1	76116128	1174.4
plastid_rada_mut_2	68615282	871.7

plastid_rada_mut_3	45985626	1068.7
plastid_rada_wild_1	53480887	234.2
plastid_rada_wild_2	46684396	954.5
plastid_rada_wild_3	46190084	776.4
plastid_reca1_mut_1	66804365	543.7
plastid_reca1_mut_2	38396319	594.8
plastid_reca1_mut_3	30645358	299.3
plastid_reca1_wild_1	37377457	598.2
plastid_reca1_wild_2	32420159	543.5
plastid_reca1_wild_3	33351491	331.1

Table S3. Results from Kruskal-Wallis test comparing SNV frequencies among genomic regions in WT and *msh1* mutant data from Wu *et al.,* (2020)

Sample	**Kruskal-Wallis chi-squared value**	**p-value**
msh1 mitochondria	6.03	0.19
msh1 plastid	5.47	0.24
WT mitochondria	6.66	0.15
WT plastid	11.35	0.02

758 **Table S4.** Oxford Nanopore sequencing yields for each of the three runs

Sample	Sequencing run	Read count	Long reads count (>500bp)	Total yield (Mb)
plastid_recA1_wild_1	1	224238	131719	412.21
plastid_recA1_mut_1	1	82051	39041	121.45
plastid_recA1_mut_2	1	74341	32851	130.77
plastid_recA1_mut_3	1	72833	41137	167.30
plastid_radA_wild_1	1	127499	85335	307.34
plastid_radA_mut_1	1	111390	72395	297.02
plastid_radA_mut_3	1	186393	119090	540.66
plastid_osb2_wild_3	1	101793	66081	239.62
plastid_osb2_mut_1	1	143806	92534	407.94
plastid_osb2_mut_2	1	103151	74649	349.70
plastid_osb2_mut_3	1	109492	63761	260.72
plastid_msh1_wild_3	1	45501	29533	126.16
plastid_msh1_mut_1	1	36518	24441	111.72
plastid_msh1_mut_2	1	46533	26330	97.91
plastid_msh1_mut_3	1	47757	32369	153.13
mitochondrial_recA3_wild_1	2	8481	6019	56.73
mitochondrial_recA3_mut_1	2	1442	813	8.70
mitochondrial_recA3_mut_2	2	20256	14861	101.19
mitochondrial_recA3_mut_3	2	13261	8069	52.79
mitochondrial_radA_wild_3	2	2119	766	4.64
mitochondrial_radA_mut_1	2	13790	6079	22.39
mitochondrial_radA_mut_2	2	3675	154	0.90
mitochondrial_radA_mut_3	2	1384	681	6.32
mitochondrial_why2_wild_1	2	4720	2629	20.01

mitochondrial_why2_mut_1	2	9965	6992	50.01
mitochondrial_why2_mut_2	2	1112	411	3.34
mitochondrial_why2_mut_3	2	1279	287	2.78
mitochondrial_MSH1_wild_1	2	931	95	0.52
mitochondrial_MSH1_mut_1	2	959	151	0.64
mitochondrial_MSH1_mut_2	2	925	50	0.42
mitochondrial_MSH1_mut_3	2	471	34	0.22
mitochondrial_recA3_wild_1	3	16270	12616	120.48
mitochondrial_recA3_mut_1	3	1684	1028	11.65
mitochondrial_recA3_mut_2	3	13791	10705	97.58
mitochondrial_recA3_mut_3	3	13488	9944	82.53
mitochondrial_radA_wild_3	3	869	650	3.98
mitochondrial_radA_mut_1	3	18460	13217	53.96
mitochondrial_radA_mut_2	3	393	44	0.19
mitochondrial_radA_mut_3	3	1017	500	5.02
mitochondrial_why2_wild_1	3	3596	2496	18.99
mitochondrial_why2_mut_1	3	6147	3618	26.85
mitochondrial_why2_mut_2	3	1507	85	0.62
mitochondrial_why2_mut_3	3	508	92	0.77

Note that, for the *radA* mtDNA analysis, we averaged structural variant frequencies and coverages across the mitochondrially and plastid-derived samples, while for *msh1,* we relied entirely on the plastid-derived samples and did not investigate the mitochondrially derived samples, which had extremely low yield.

759 **Table S5.** Sequencing depth per bp (calculated with bedtools depth) of samples in Fig 8.

Sample	Sequencing protocol	Mutant (total cov/bp)	WT (total cov/bp)
radA_mito	nanopore	222.9	101.6
recA3_mito	nanopore	736.4	372.1
why2_mito	nanopore	170.9	82.5
msh1_mito	nanopore	161.9	36.9
radA_mito	duplex	1600.2	1377.4
recA3_mito	duplex	941.4	647.8
why2_mito	duplex	1058.7	1235.2
msh1_mito	duplex	1020.9	1209.6
msh1_plastid	nanopore	1650.1	762.0
osb2_plastid	nanopore	6862.2	1663.7
radA_plastid	nanopore	5514.3	1668.5
recA1_plastid	nanopore	2422.6	2603.1
msh1_plastid	duplex	1754.4	1645.3
osb2_plastid	duplex	3244.9	3009.4
radA_plastid	duplex	3444.6	2205.6
recA1_plastid	duplex	1606.6	1650.2

760

APPENDIX FOR SUPPLEMENTARY FILES

FileS1_mutation_counts: Coverages, mutation counts, and variant frequencies from the Duplex Sequencing analysis of data generated in this study and in Wu *et al.,* 2020.

FileS2_repeat_recomb_freq_mito: Counts of recombined reads and total repeat spanning reads used to calculate repeat specific recombination frequencies. We focused our mitochondrial analysis on repeats which has at least 10 recombined reads (across all replicates)**.**

FileS3_repeat_recomb_freq_plastid: Counts of recombined reads and total repeat spanning reads used to calculate repeat specific recombination frequencies. We focused our plastid analysis on repeats which has at least 3 recombined reads (across all replicates)**.**